2022 First International Conference on Electrical, Electronics, Information and Communication Technologies (ICEEICT) | 978-1-6654-3647-2/22/$31.00 ©2022 IEEE | DOI: 10.1109/ICEEICT53079.2022.9768415

System-on-chip based Automated Optic Disk Segmentation in Retinal Images

Neelapala Anil Kumar
Alliance University
Bengaluru, India 562 106
Email: elegantanil2008@gmail.com

Gnane Swarnadh Satapathi
A J Institute of Engineering and Technology
Mangalore, India 575 006
Email: gnaneswarnadhsatapathi@ajiet.edu.in

Mosa Satya Anuradha
Andhra University

***Abstract*—In this paper a novel technique on automated optical disk (OD) segmentation is proposed. The proposed OD algorithm depends on morphological based algorithm. This technique is assessed on openly accessible standard data sets DRIONS. The average accuracy rate of proposed segmented technique is 97.6% on DRIONS database. The proposed algorithm achieved Average Sensitivity, Average Specificity and Average Overlap of 93.1%, 98.4% and 86.3% respectively on DRIONS data sets. Test results shows the algorithm is superior with comparable execution time over existing OD algorithms. Further, the algorithm has been implemented in System-on-chip (Zync-7000) kit.**

***Index Terms*—Diabetic Retinopathy, Morphological Operation, Optic disk, Retinal image.**

I. Introduction

Diabetic retinopathy is a conventional retinal problem related with diabetes. Typical retinal pictures comprises of fovea, blood vessels and optical disk (OD). The blood vessels of the retina start from OD. The features like location, size and appearance of OD can determine some of the retinal disorders. So, there is a need to determine the features to diagnose the retinal disorders. Further, lesions and OD appears to be bright in color, and there could be a chance of classification. Therefore, OD segmentation plays an crucial role for identifying the diseases like Glaucoma and diabetic retinopathy. In addition to it, OD segmentation also assist in computing extra features like macula and fovea.

There are numerous techniques suggested for confinement of optical disk in retinal pictures. The OD identification technique suggested by [1], uses vessel back-tracking mechanism to their starting point. The technique is absolutely probably the most secure method for confining the OD, however it is intensely dependent on correct vessel recognition. A subimage is utilized to compute the intensity variation of near by pixels and the point with highest intensity variation is considered as OD center [2]. But, this method fails when there is huge number of dominant vessels and white lesions. The OD is localized by utilizing pyramidal decomposition and Hausdorff based template correlative algorithm [3].

Sobel operators and Hough transform is proposed for detecting the outer ring of OD and its center respectively in [4]. By using this technique, 90% progress rate was achieved especially for DRIVE dataset. A strategy dependent on connected component analysis and iterative thresholding is suggested to distinguish the estimated focal point of the OD [5]. Iterative technique is used to determine the boundary of OD, but the iteration loop has to be continued until its optimal. Disk-shape of OD is computed using morphological operations and Hough transform in [6], [7], [8]. A new technique is suggested to calculate the boundary of OD by detecting the vessels in [9]. Vasculature OD properties and Bayesian classifier is utilized to discover the OD in retinal pictures is prposed in [10].

Active contours and morphological operations are employed to track the OD is suggested in [11], [14]. The OD region and boundary is detected by using modified variance image algorithm in [12], [13]. Watershed algorithm and local grey level variation algorithm is used to detect boundary and center of OD respectively. Iterative thresholding, roundness and Hough transform is used to detect the boundary and center of OD in [7]. The best disk shape of OD is detected by using regression based algorithm and texture descriptors [15]. Color morphology is utilized to separate the blood vessels from OD and maximum variance algorithm is used to compute the center of OD in [16]. Morphological operators are suggested to detect the OD boundary in [17], [18], [19]. The majority of the techniques ([20], [21], [22], [23], [24]) in the writing distinguishes just focus on the OD. Practically all OD identification and division techniques in writing depended on preprocessing and huge number of calculations. Thus computational intricacy is high. Moreover, the techniques proposed in literature didn't propose the execution feasibility of algorithm in hardware. In this paper, morphological operation based automated optical disk detection with low computational complexity and less execution time is proposed. Further, the proposed algorithm is written in MATLAB and converted into VHDL code using HDL converter and executed in Xilinx Zynq-7000 SOC kit.

The paper is coordinated as follows: Proposed technique is explained in Section II. Simulation results and detailed discussion are introduced in Section III. Section IV depicts conclusion.

II. Proposed Approach

The proposed approach of automated optical disk segmentation is divided into three subsections

- Pre-processing
- Localization of optical disk center

- Segmentation of optical disk

A. Pre-processing

Preprocessing and removal of blood vessels perform an important task in localization and segmentation of optical disk (OD). The optical disk consists of bright intensity pixels in red channel as well as green channel of the retinal fundus image. However, the green channel of the fundus image has highest contrast when compared to blue and red channel of the image. Hence, green channel is selected for segmenting the optical disk. To further increase the contrast of green channel image, adaptive histogram equalization is performed [25].

The intensity values of both optical disk and lesions are identical. Due to this uncertainty, there will be difficulty while classifying lesion, OD region and vice versa. The only difference between lesion and OD region is the pixel size. So, mean filtering is applied to the histogram equalized green fundus image to remove the lesion. The mean filter will eliminate the pixel values which are different from their surrounding pixels. A kernel of size 3×3 is considered and is convoluted with the input image so as to remove lesion. The filtered image ($I^{filter}_{x,y}$) is given as

$$I^{filter}_{x,y} = I_{x,y} \otimes K \tag{1}$$

where, $I_{x,y}$ = adaptive histogram equalized green fundus image and K is kernel, which is depicted as

$$K = \frac{1}{9}\begin{bmatrix} 1 & 1 & 1 \\ 1 & 1 & 1 \\ 1 & 1 & 1 \end{bmatrix} \tag{2}$$

The filtered image ($I^{filter}_{x,y}$) is ready either for localizing the optic disk center otherwise for segmenting optic disk boundary.

B. Localization of OD center

The output of mean filtering is a blurred image where white intensity regions can be seen evidently. All the intensity pixels of filtered image are arranged in declined order. The first intensity value is considered as the maximum intensity value ($I^{max}_{x,y}$) and is utilized as a reference point. The mean value ($I^{mean}_{x,y}$) is computed by employing the mean function on surrounding pixels of the reference value ($I^{max}_{x,y}$). If the surrounding pixel size is considered as $S \times T$, then the mean value is given as

$$I^{mean}_{x,y} = \frac{1}{ST} \sum_{x-\frac{S}{2}}^{x+\frac{S}{2}} \sum_{y-\frac{S}{2}}^{y+\frac{S}{2}} p_{x,y} \tag{3}$$

where, S, T are number of rows and columns respectively, $p_{x,y}$ is the pixel value.

The segmented binary image is obtained by $I^{B}_{x,y}$ is obtained by thresholding the mean filtered image ($I^{filter}_{x,y}$) which is given as

$$I^{B}_{x,y} = \begin{cases} 1 & \text{if } I^{filter}_{x,y} \geq I^{mean}_{x,y} \\ 0 & otherwise \end{cases} \tag{4}$$

The binary image $I^{B}_{x,y}$ might comprise of one or more connected components (C^c) which is given as

$$I^{B}_{x,y} = \cup^{a\$b} C^a, C^c \cap C^d = 0; \forall_{c,d \varepsilon b}; c \quad d \tag{5}$$

where, $b = 1, 2, 3, \ldots, a$ represents the number of connected components in binary image, $C^c \cap C^d = 0$ states that two connected regions are not overlapped each other, $\cup^{a\$b} C^a$ represents that there are a regions in binary image $I^{B}_{x,y}$ $\forall_{c,d \varepsilon b}$ represents that both the regions c and d of $I^{B}_{x,y}$ belongs to b, $c = d$ represents that, c and d are dissimilar region.

The circular shaped component in C^a is considered as optical disc region and this component has the wide number of connected pixels. The circular shaped component is located by calculating compactness feature [26] and is given as

$$C(C^a) = \frac{4\pi \mathrm{N}(C^a)}{a^2(C^a)} \tag{6}$$

where, a represents number of connected components, C^a indicates a^{th} connected component, $C(C^a)$ represents the compactness feature of a^{th} connected component, N shows the number of pixels lies in a^{th} region and $a(C^a)$ represents the number of pixels surrounding C^a.

The values of compactness are organized in decreasing order and the first value (largest value) of component will be the optical disk position of the fundus image. The centroid of the largest connected component is computed and is designated as center of the optical disk.

C. Optical Disk Segmentation

After applying mean filter to the adaptive histogram equalized image, the blood vessels are removed. But, there might be bright small lesions along with boundary and these are eliminated by performing morphological operation. Morphological disk erosion and dilation operations are performed on the mean filtered image. The radius of the structuring disk element are evaluated experimentally. Better results were obtained if the radius size is almost equal to half of factual size of the optic disk. The erosion operation narrows the bright components by eliminating the boundary pixels. The entire boundary pixels are removed after performing dilation operation. The equations for erosion and dilation is given as

$$I^{ero}_{x,y} = min_{m,n \varepsilon S^1} \; I^{filter}_{x-m,y-n} + S^1_{m,n} \tag{7}$$

$$I^{dil}_{x,y} = max_{m,n \varepsilon S^2} \; I^{ero}_{x-m,y-n} + S^2_{m,n} \tag{8}$$

where, $I^{ero}_{x,y}$, $I^{dil}_{x,y}$ represents eroded and dilated image respectively; S^1, S^2 represents disk structuring element of erosion and dilation respectively.

After performing dilation procedure, the optic disk can be seen clearly. For acquiring the actual shape of optic disk and smoothing the edges, median filter is applied. Any small bright regions can be further removed by using thresholding technique. Sobel edge detection technique is applied to the thresholded image for attaining boundary of the optical disk. The boundary of optical disk is now superimposed on original image of fundus component so as to check the accuracy.

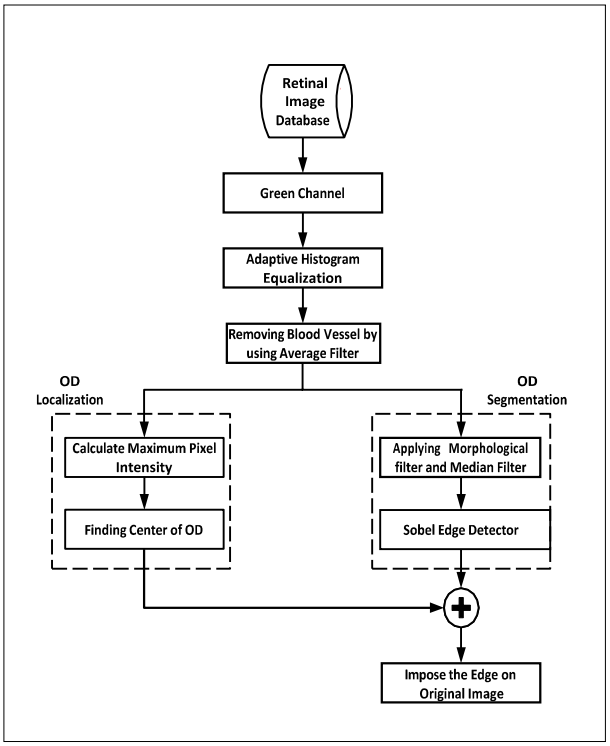

Fig. 1: Proposed Optical Disk Segmentation Algorithm

III. Experimental Results and Discussion

The performance of the proposed technique is computed on benchmark DRIONS retinal image database [31]. The DRIONS database comprises of 110 images with size and Field of View (FOV) of 400×600 pixels and 50 respectively. The images were obtained with color analogical fundus camera by centering the head of optic nerve. Further, the images were digitized by employing a HP-PhotoSmart-S20 high-resolution scanner with quantization level of 8 bits/pixel.

The segmentation and preprocessing code of optical disk is written in MATLAB associated with test bench. The preprocessing subsection is performed in test bench and the mean filtered output is sent to the MATLAB function in the form of pixel stream. The MATLAB coder converts the pixel values into fixed precision floating point format as per the requirement of hardware. Further, the HDL coder converts the MATLAB function into VHDL code. Once the HDL code is synthesized, a bit file is generated and is dumped into the SOC kit (Xilinx Zynq®-7000). All the operations necessary for performing morphological dilation, erosion, median filtering and edge detection are managed by HDL coder itself.

Average sensitivity, average accuracy, average predicted value, average specificity, average overlap and average computation time are the metrics considered to examine the performance of the proposed technique. The metrics are illustrated as

$$Sensitivity = \frac{TP}{TP + FN} \tag{9}$$

$$PredictedV alue = \frac{TP}{TP + FP} \tag{10}$$

$$Specificity = \frac{TN}{TN + FN} \tag{11}$$

$$Accuracy = \frac{TP + TN}{\text{Total number of images in database}} \tag{12}$$

$$Overlap = \frac{area\,(A \cap B)}{area\,(A \cup B)} \tag{13}$$

where TP, TN, FP and FN are true positive, true negative, false positive and false negative pixels respectively. Parameters A and B corresponds to manually acquired optic disk and proposed algorithm calculated optic disk region respectively.

Figure 2 exhibits the result of suggested technique. Figure 2b is the green channel component of the original input image (Figure 2a). To increase the contrast of green channel component, adaptive histogram equalization is performed whose result is depicted in Figure 2c. Lesions are removed by applying average filter and the output of mean filter image is portrayed in Figure 2d. Further, lesions are removed by using morphological operations and the result is illustrated in Figure 2f. The boundary of the optical disk is computed by using Sobel edge detector (Figure 2g). The center of optical disk is shown in Figure 2e. Eventually, the boundary and center of optical disk is superimposed on the original input image which is illustrated in Figure 2h.

The comparative study for detecting optical disk of proposed algorithm with available methods is illustrated in Table I. The proposed method has comparable accuracy with existing algorithms [20], [27], [28], [29], [30] and has 2.16% percent high accuracy when compared to [21]. Further, the average sensitivity of the suggested technique is 0.7% and 9% high when compared to [30] and [21] respectively. Similarly, the average overlap is 5.2%, 2.37%, 5.1% and 1.49% higher when compared to [20], [27], [30], [21] respectively. The average computation time is 60.3% and 71.4% less when compared to [20] and [21] respectively. The previous studies ignored the average predicted value and found to be 91.5%. The average predicted values gives the information about exact boundaries that is identified. Table II shows the HDL utilization report for detecting optical disk. The results suggest that the proposed technique has approximated outputs when compared to state-of-art optical disk segmentation algorithms except [30]. But, there lies difficulty (in terms of computation complexity) while applying the circular hough transform in real time hardware. So, the proposed technique can be employed for automated optical disk segmentation for retinal images.

IV. Conclusion and Future Work

In this paper a novel technique on automated optical disk (OD) segmentation is introduced. The proposed OD algorithm depends on morphological based technique and this algorithm is assessed on openly accessible standard data sets DRIONS. The average accuracy rate of proposed segmented technique is 97.6% on DRIONS database. The proposed algorithm achieved Average Sensitivity, Average Specificity and Average

TABLE I: Comparison of performance metrics for proposed algorithm with state-of-art optical disk segmentation techniques

Method	Average Accuracy	Average Sensitivity	Average Specificity	Average Predictive Value	Average Overlap	Average Computation Time (in sec)
Rehman et al. [20]	0.9930	0.9480	0.9940	-	0.8210	31.10
Fan et al. [27]	0.9760	-	-	-	0.8473	-
Zahoor et al. [28]	0.9986	0.9384	0.9994	-	0.8862	1.60
Morales et al. [29]	0.9934	-	-	-	-	-
Ramani et al. [30]	0.9937	0.9249	0.9959	-	0.8217	1.41
Abdullah et al.[21]	0.9549	0.8508	0.9966	-	0.8510	43.20
Proposed Method	0.976	0.931	0.984	0.915	0.8637	12.33

(a) Input Image

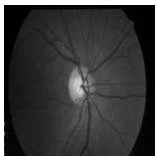

(b) Green Channel

(c) Adaptive Histogram Equalized Image

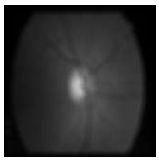

(d) Average Filtered image

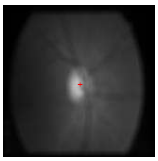

(e) Center of Optical Disk

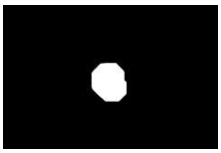

(f) Image after morphological operation

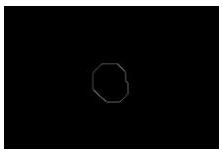

(g) Sobel Edge deteor

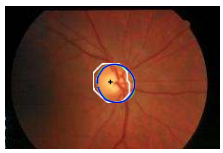

(h) Optical Disk superimposed with OD center on Original Image

Fig. 2: Optic Disk Segmentation

TABLE II: HDL Resource Utilization Report

Hardware Summary	Count
Multipliers	162
Adders/ Subtractors	246
Registers	711
Total 1 bit Registers	4661
RAMS	6
Multiplexers	307
I/O Bits	52
Shifters	1

Overlap of 93.1%, 98.4% and 86.3% respectively on DRIONS data sets. Test results show the superior performance with comparable execution time over existing OD algorithms. Further, the algorithm has been implemented in System-on-chip (Zync-7000) kit. In future, the algorithm has to be tested on more datasets like DRIVE, DIRATEDB0 and DIRATEDB1.

REFERENCES

[1] K. Akita and H. Kuga, "Pattern recognition of blood vessel networks in ocular fundus images," in *Medical Imaging and Image Interpretation*, vol. 375. International Society for Optics and Photonics, 1982, pp. 436–443.

[2] C. Sinthanayothin, J. F. Boyce, H. L. Cook, and T. H. Williamson, "Automated localisation of the optic disc, fovea, and retinal blood vessels from digital colour fundus images," *British journal of ophthalmology*, vol. 83, no. 8, pp. 902–910, 1999.

[3] M. Lalonde, L. Gagnon, and M.-C. Boucher, "Non-recursive paired tracking for vessel extraction from retinal images," in *Vision interface*, 2000, pp. 61–68.

[4] X. Zhu, R. M. Rangayyan, and A. L. Ells, "Detection of the optic nerve head in fundus images of the retina using the hough transform for circles," *Journal of digital imaging*, vol. 23, no. 3, pp. 332–341, 2010.

[5] P. Siddalingaswamy and K. G. Prabhu, "Automatic localization and boundary detection of optic disc using implicit active contours," *International Journal of Computer Applications*, vol. 1, no. 7, pp. 1–5, 2010.

[6] M. Niemeijer, B. van Ginneken, and M. D. Abràmoff, "Automatic detection of the optic disc, fovea and vacular arch in digital color photographs of the retina." in *BMVC*, 2005.
[7] M. Park, J. S. Jin, and S. Luo, "Locating the optic disc in retinal images," in *International Conference on Computer Graphics, Imaging and Visualisation (CGIV'06)*. IEEE, 2006, pp. 141–145.
[8] S. Sekhar, W. Al-Nuaimy, and A. K. Nandi, "Automated localisation of retinal optic disk using hough transform," in *2008 5th IEEE international symposium on biomedical imaging: from nano to macro*. IEEE, 2008, pp. 1577–1580.
[9] F. Ter Haar, "Automatic localization of the optic disc in digital colour images of the human retina," *Utrecht University*, 2005.
[10] K. W. Tobin Jr, E. Chaum, V. P. Govindasamy, T. P. Karnowski, and O. Sezer, "Characterization of the optic disc in retinal imagery using a probabilistic approach," in *Medical Imaging 2006: Image Processing*, vol. 6144. International Society for Optics and Photonics, 2006, p. 61443F.
[11] F. Mendels, C. Heneghan, and J. Thiran, "Identification of the optic disk boundary in retinal images using active contours," in *Proceedings of Irish Machine Vision and Image Processing Conference (IMVIP) 1999*, no. CONF. IEEE, 1999, pp. 103–115.
[12] T. Walter and J.-C. Klein, "Segmentation of color fundus images of the human retina: Detection of the optic disc and the vascular tree using morphological techniques," in *International symposium on medical data analysis*. Springer, 2001, pp. 282–287.
[13] T. Walter, J.-C. Klein, P. Massin, and A. Erginay, "A contribution of image processing to the diagnosis of diabetic retinopathy-detection of exudates in color fundus images of the human retina," *IEEE transactions on medical imaging*, vol. 21, no. 10, pp. 1236–1243, 2002.
[14] A. Sopharak, B. Uyyanonvara, and S. Barman, "Automatic exudate detection from non-dilated diabetic retinopathy retinal images using fuzzy c-means clustering," *sensors*, vol. 9, no. 3, pp. 2148–2161, 2009.
[15] C. A. Lupascu, D. Tegolo, and L. Di Rosa, "Automated detection of optic disc location in retinal images," in *2008 21st IEEE International Symposium on Computer-Based Medical Systems*. IEEE, 2008, pp. 17–22.
[16] G. B. Kande, P. V. Subbaiah, and T. S. Savithri, "Segmentation of exudates and optic disk in retinal images," in *2008 Sixth Indian Conference on Computer Vision, Graphics & Image Processing*. IEEE, 2008, pp. 535–542.
[17] D. Welfer, J. Scharcanski, and D. R. Marinho, "A morphologic two-stage approach for automated optic disk detection in color eye fundus images," *Pattern Recognition Letters*, vol. 34, no. 5, pp. 476–485, 2013.
[18] J. Seo, K. Kim, J. Kim, K. Park, and H. Chung, "Measurement of ocular torsion using digital fundus image," in *The 26th Annual International Conference of the IEEE Engineering in Medicine and Biology Society*, vol. 1. IEEE, 2004, pp. 1711–1713.
[19] K. Stapor, A. Świtonski, R. Chrástek, and G. Michelson, "Segmentation of fundus eye images using methods of mathematical morphology for glaucoma diagnosis," in *International Conference on Computational Science*. Springer, 2004, pp. 41–48.
[20] Z. U. Rehman, S. S. Naqvi, T. M. Khan, M. Arsalan, M. A. Khan, and M. Khalil, "Multi-parametric optic disc segmentation using superpixel based feature classification," *Expert Systems with Applications*, vol. 120, pp. 461–473, 2019.
[21] M. Abdullah, M. M. Fraz, and S. A. Barman, "Localization and segmentation of optic disc in retinal images using circular hough transform and grow-cut algorithm," *PeerJ*, vol. 4, p. e2003, 2016.
[22] S. Bharkad, "Automatic segmentation of optic disk in retinal images," *Biomedical Signal Processing and Control*, vol. 31, pp. 483–498, 2017.
[23] S. D. Bharkad, "Automatic segmentation of optic disk in retinal images using dwt," in *2016 IEEE 6th International Conference on Advanced Computing (IACC)*. IEEE, 2016, pp. 386–391.
[24] H. M. Ünver, Y. Kökver, E. Duman, and O. A. Erdem, "Statistical edge detection and circular hough transform for optic disk localization," *Applied Sciences*, vol. 9, no. 2, p. 350, 2019.
[25] S. M. Pizer, E. P. Amburn, J. D. Austin, R. Cromartie, A. Geselowitz, T. Greer, B. ter Haar Romeny, J. B. Zimmerman, and K. Zuiderveld, "Adaptive histogram equalization and its variations," *Computer vision, graphics, and image processing*, vol. 39, no. 3, pp. 355–368, 1987.
[26] S. J. Ahn, W. Rauh, and S. I. Kim, "Circular coded target for automation of optical 3d-measurement and camera calibration," *International Journal of Pattern Recognition and Artificial Intelligence*, vol. 15, no. 06, pp. 905–919, 2001.
[27] Z. Fan, Y. Rong, X. Cai, J. Lu, W. Li, H. Lin, and X. Chen, "Optic disk detection in fundus image based on structured learning," *IEEE journal of biomedical and health informatics*, vol. 22, no. 1, pp. 224–234, 2017.
[28] M. N. Zahoor and M. M. Fraz, "Fast optic disc segmentation in retina using polar transform," *IEEE Access*, vol. 5, pp. 12 293–12 300, 2017.
[29] S. Morales, V. Naranjo, J. Angulo, and M. Alcañiz, "Automatic detection of optic disc based on pca and mathematical morphology," *IEEE transactions on medical imaging*, vol. 32, no. 4, pp. 786–796, 2013.
[30] R. G. Ramani and J. J. Shanthamalar, "Improved image processing techniques for optic disc segmentation in retinal fundus images," *Biomedical Signal Processing and Control*, vol. 58, p. 101832, 2020.
[31] J. Feijoo, J. de la Casa, H. Servet, M. Zamorano, M. Mayoral, and E. Suárez, "Drions-db: digital retinal images for optic nerve segmentation database," 2014.